

EUR 3881 e

European Atomic Energy Community - EURATOM

FIAT SpA, Sezione Energia Nucleare - Torino

Società ANSALDO SpA - Genova

**FORCED CONVECTION BURNOUT AND
HYDRODYNAMIC INSTABILITY
EXPERIMENTS
FOR WATER AT HIGH PRESSURE**

**Part IV : BURNOUT EXPERIMENTS IN A DOUBLE CHANNEL TEST
SECTION WITH TRANSVERSELY VARYING HEAT GENERATION**

by

**A. CAMPANILE, G. GALIMI and M. GOFFI
(SORIN, Centro Ricerche Nucleari, Saluggia-Italy)**

1968



Contract No. 008-61-12-PNII

LEGAL NOTICE

This document was prepared under the sponsorship of the Commission of the European Communities.

Neither the Commission of the European Communities, its contractors nor any person acting on their behalf :

Make any warranty or representation, express or implied, with respect to the accuracy, completeness, or usefulness of the information contained in this document, or that the use of any information, apparatus, method, or process disclosed in this document may not infringe privately owned rights ; or

Assume any liability with respect to the use of, or for damages resulting from the use of any information, apparatus, method or process disclosed in this document.

This report is on sale at the addresses listed on cover page 4

at the price of FF 5.—	FB 50.—	DM 4.—	Lit. 620	Fl. 3.60
------------------------	---------	--------	----------	----------

When ordering, please quote the EUR number and the title, which are indicated on the cover of each report.

Printed by Vanmelle S.A.
Brussels, February 1968

This document was reproduced on the basis of the best available copy.

EUR 3881 e

FORCED CONVECTION BURNOUT AND HYDRODYNAMIC INSTABILITY EXPERIMENTS FOR WATER AT HIGH PRESSURE
Part IV : BURNOUT EXPERIMENTS IN A DOUBLE CHANNEL TEST SECTION WITH TRANSVERSELY VARYING HEAT GENERATION

by A. CAMPANILE, G. GALIMI and M. GOFFI (SORIN, Centro Ricerche Nucleari, Saluggia — Italy)

European Atomic Energy Community — EURATOM

FIAT SpA, Sezione Energia Nucleare — Torino

Società ANSALDO SpA — Genova

Contract No. 008-61-12 PNII

Brussels, February 1968 — 36 Pages — 13 Figures — FB 50

Experiments have been carried out on a complex geometry test section consisting of two heating rods coaxially mounted in two adjacent and communicating flow channels.

EUR 3881 e

FORCED CONVECTION BURNOUT AND HYDRODYNAMIC INSTABILITY EXPERIMENTS FOR WATER AT HIGH PRESSURE
Part IV : BURNOUT EXPERIMENTS IN A DOUBLE CHANNEL TEST SECTION WITH TRANSVERSELY VARYING HEAT GENERATION

by A. CAMPANILE, G. GALIMI and M. GOFFI (SORIN, Centro Ricerche Nucleari, Saluggia — Italy)

European Atomic Energy Community — EURATOM

FIAT SpA, Sezione Energia Nucleare — Torino

Società ANSALDO SpA — Genova

Contract No. 008-61-12 PNII

Brussels, February 1968 — 36 Pages — 13 Figures — FB 50

Experiments have been carried out on a complex geometry test section consisting of two heating rods coaxially mounted in two adjacent and communicating flow channels.

Several conditions of differential heating in the two channels were tested to the aim of investigating the effect on burnout limits of possible variations of local flow velocity and fluid enthalpy due to transverse flow redistribution and mixing.

Several conditions of differential heating in the two channels were tested to the aim of investigating the effect on burnout limits of possible variations of local flow velocity and fluid enthalpy due to transverse flow redistribution and mixing.

EUR 3881 e

European Atomic Energy Community - EURATOM

FIAT SpA, Sezione Energia Nucleare - Torino

Società ANSALDO SpA - Genova

**FORCED CONVECTION BURNOUT AND
HYDRODYNAMIC INSTABILITY
EXPERIMENTS
FOR WATER AT HIGH PRESSURE**

**Part IV : BURNOUT EXPERIMENTS IN A DOUBLE CHANNEL TEST
SECTION WITH TRANSVERSELY VARYING HEAT GENERATION**

by

**A. CAMPANILE, G. GALIMI and M. GOFFI
(SORIN, Centro Ricerche Nucleari, Saluggia-Italy)**

1968



Contract No. 008-61-12-PNII

SUMMARY

Experiments have been carried out on a complex geometry test section consisting of two heating rods coaxially mounted in two adjacent and communicating flow channels.

Several conditions of differential heating in the two channels were tested to the aim of investigating the effect on burnout limits of possible variations of local flow velocity and fluid enthalpy due to transverse flow redistribution and mixing.

KEYWORDS

HEATING
BURNOUT
MOCKUP
FLUID FLOW

ENTHALPY
VELOCITY
COOLANT LOOPS
TESTING

TABLE DES MATIERES

	Page
1. Introduction	5
2. Test section	5
3. Control of the subchannels geometrical symmetry . .	8
4. Burnout experiments	10
4.1. Range of parameters	10
4.2. Burn-out data presentation	10
5. Remarks.	11
Bibliography	14

FORCED CONVECTION BURNOUT AND HYDRODYNAMIC INSTABILITY EXPERIMENTS
FOR WATER AT HIGH PRESSURE⁽⁺⁾

1. Introduction

The flow passage of an open lattice core, with rod bundle type fuel elements, consists of non circular channels bounded by fuel rods each having connections with the neighbouring channels through the gap between the rods.

Several factors may contribute to set-up non uniform transverse conditions in a matrix of fuel rods and coolant channels, namely:

- Radial flux distribution
- Flux peaking
- Dimensional tolerances and deformations
- Fuel loading variations
- Inlet flow differences
- Presence of non fueled rods (cluster control).

To the purpose of investigating possible influences of transversally unbalanced conditions existing in adjacent channels an experimental study has been carried-out by SORIN under the research and development contract between EURATOM-FIAT and Ansaldo for nuclear ship propulsion.

The experiments were performed on the SORIN pressurized water loop described in detail in ref. [1].

Fig. 1 shows a schematic diagram of the loop.

2. Test section

The investigation on the influence of transverse shift of flow upon the burnout in subchannels of a rod cluster fuel

⁽⁺⁾ Manuscript received on December 12, 1967.

assembly, was performed in a test section consisting of two adjacent and communicating channels with provision for differential heating in the two channels.

Each channel had a heater rod in axial position. The perimetral contour of the flow duct, hereafter referred to as the shell, was shaped as to simulate the configuration of the flow area associated with two fuel rods in a rod bundle (Fig. 2). It was suitably designed to have heat generation practically in the curved section only of the containment wall.

This was achieved by brazing, in a controlled atmosphere furnace, four quarters and two halves of stainless steel tubes, 1 mm thick, to very thin stainless steel strips, 0.18 mm thick.

The corrugation of the thin strips observed in the preliminary specimens [2] was considerably reduced by improving the technique of fastening the various parts in the furnace.

Stainless steel discs were brazed at each end of the shell to allow connection to the electrical power connectors.

The heater rods consisted of two stainless steel tubes 10.2 mm O.D., 1 mm thick, internally provided with four thin stainless steel wires welded to the tube walls at the entrance, the exit, the mid point and 10 mm upstream of the exit end of the heated length. The wires were used as voltage taps for voltage drop measurement as well as for burnout detection by means of a bridge type detector .

The heater rods were centralized in each subchannel by passing them through positioning holes of an entry and exit grid plates. All the parts at different voltage were suitably insulated by using sintered aluminium oxide rings.

In addition, to eliminate the risk for the rods to get in touch with perimetral walls, each of them was held in position by means of two sets of three adjustable ceramic pins at 120° located at 1/3 and 2/3 of the entire heated length (Fig. 3).

The heating current to the three resistors of the test channel, namely the two rods and the shell, was supplied from a d-c rectifier rated for 600 kW.

The rod purposely selected to be overloaded up to the burnout threshold, hereafter referred to as "burnout rod", was spring loaded to prevent it from bowing during the burnout tests.

In order to obtain present ratios of the shell and adjacent rod heat flux to burnout rod heat flux, provision was made to allow feeding of the heating elements at different voltage through a suitable setting of the variable resistors R_1 and R_2 (Fig. 4).

The electrical connectors were made of stranded copper cable enclosed in flexible stainless steel corrugated tubes. This arrangement presented enough flexibility to leave the heated elements free to expand.

The channel, with the rods positioned in the end terminal grid plates, was enclosed in a thin cylindrical shell, and the space in between was filled with aluminum oxide fragments to the purpose of thermally insulating the channel and preventing intense convection of the stagnant external water. Fig. 5 shows a close-up view of the exit section of the channel.

The entire assembly was inserted in a test section housing designed to withstand the pressure.

The housing was made of a 4" schedule 80 stainless steel pipe connecting two terminal stainless steel heads machined to provide flanged electrically insulated passages for the electrical connectors.

The manufacturing difficulties of the channel and the limited size of the controlled atmosphere furnace, reduced the available heated length of the test section to 590 mm.

Water flow was measured by a turbine flow meter as well as an orifice plate, the former allowing recording of the water flow signals.

Two sheat type thermocouples were used for water inlet temperature measurements, whereas five thermocouple of the same type were located at different positions of the exit flow area enabling an evaluation of the water temperature tranverse distribution.

Fig. 6 indicate the relevant dimensions of the channel flow area and the positions of the five thermocouples located at the channel exit.

3. Control of the subchannels geometrical symmetry

The tests preliminary performed and referred to in a previous paper [2], were considered as a check on the overall feasibility of the mixing experiments in the designed test apparatus.

In fact, in the course of the above runs, a primary tranverse geometrical asymmetry was discovered in the two adjacent channels through the check of some distributions of the exit water temperatures over the flow area obtained from experiments

with symmetric heat generation.

This primary asymmetry could be charged to several geometrical imperfections observed in the earlier prototypes of the channel.

The improvement of the manufacturing technique of the channel and the use of a second set of ceramic spacers, allowed to achieve the symmetry requirements for the complex flow passage in cold conditions. As a check of the overall reliability of the experimental set up in hot conditions, tests were made aiming at the control of channel symmetry with the fluid circulating at the operating pressure and temperature.

In these check runs the water exit temperature distribution was assumed as experimental evidence of the transverse symmetry of the system.

The following check tests were performed:

- steady-state tests with heating limited alternatively to the two rods.
- steady-state tests with simultaneous symmetric heat generation limited to the two rods.
- steady-state test with heating limited to the channel walls only.

Figs. 7 and 8 show the results obtained for 3 typical check runs giving for each detection point of the exit flow area the ratio θ of the local to the average coolant temperature rise.

These plots show the existence of a fairly good degree of symmetry in the channel.

4. Burnout experiments

4.1. Range of parameters

The following range of parameters was covered in the present experiments:

- Mass flow rate: 49 - 230 gr/cm² sec
- Pressure : 52 - 139 ata
- Inlet temperature: 190 - 329°C.

As for the heat flux ratios, namely the burnout heater heat flux to other heaters heat flux ratio, several values were tested ranging from 0 to 1.

4.2. Burn-out data presentation

Burn-out data have been reported in Tables I through V and plotted in Fig. 9 through 13. The symbols $\Phi_{B.O.}$, Φ_A and Φ_S appearing in these representation indicate respectively:

$\Phi_{B.O.}$ = burnout heat flux of the "burnout rod"

Φ_A = heat flux of the "adjacent rod"

Φ_S = heat flux of the "shell".

The power is generated in the shell both in the curved sections as well as in the flat thin strips.

The last term contributes only for 15% of the total shell power.

As for the shell heat flux Φ_g , their values have been computed accounting only for the power and the surface of curved section of the duct.

In Fig. 9 through 13 burnout heat flux values are reported as a function of the coolant inlet temperature for the different heating conditions tested.

5. Remarks

Fig. 12 shows how, for the same inlet conditions, the heat flux on the burnout rod decreases with increasing the power generated on the shell.

Examination of the Figg. 9 through 11 suggests that, for equal inlet conditions of the coolant, the burnout heat flux on the so called "burnout rod" is unaffected by the degree of heating of the adjacent rod.

The same conclusion may be drawn from the results represented in Fig. 13.

This result could be explained assuming that a mutual compensation sets in along the channel between the effects of flow redistribution and thermal mixing.

However, the independency of the critical power on the B.O. rod with respect to the conditions in the adjacent channel, has been verified on such a large variety of coolant flow rate and enthalpy conditions, that it seems unlikely that redistribution and mixing effects might have balanced through out the tests. It is more reasonable to admit that, on short heating lengths, as the one tested in our experiments, the mixing and redistribution effects do not have any relevant

influence on the behaviour of at least a portion of the coolant cell associated to the burnout rod.

On the other hand, some experimental B.O. data of preliminary tests conducted with the test section here described, showed that the burnout heat flux on the "burnout rod" was to a certain extent affected by the degree of heating of the "adjacent rod". The trend observed was a small decrease of the burnout heat flux on the B.O. rod with increasing the heat flux of the adjacent rod.

However, in the course of the systematic experiments, whose results are here reported, this effect was never confirmed so that the preliminary data were considered rather related to some imperfections present in the first assembly.

Therefore, before drawing any conclusion on the results here reported, it is worth to obtain additional experimental evidences about the effect of transverse transport of fluid upon the critical heat flux. This work should be carried out in a different test channel, having the same lattice parameters as the one described in this report, in order to be able to find out whether the trend suggested by the data here presented is affected or not by the particular structure of the tested channel.

It is anticipated to perform experiments with transverse distribution of heat generation in a 9 rod bundle test section next to be tested in the SORIN pressurized water loop.

Acknowledgements

Appreciation is expressed for the constant cooperation of Mr. Morocutti of the Euratom.

The fruitful discussions with Mr. Previti of the FIAT Atomic Power Department are gratefully acknowledged.

Thanks are also due to the Metallurgy and Ceramics Laboratory of the FIAT APD for having made the task of brazing the various parts of the flow channel.

The authors are indebted to Mr. Bonavero, Mr. Fumero, Mr. Minazio, Mr. Passavanti and other members of the SORIN Heat Transfer Laboratory for the fine work performed throughout the present experimental program.

Finally the help offered by the SORIN workshop in manufacturing the test section is acknowledged.

Bibliography

- [1] F. Biancone, A. Campanile, G. Galimi, M. Goffi, "Forced convection burnout and hydrodynamic instability experiments for water at high pressure. Part I: Presentation of data for round tubes with uniform and non-uniform power distribution", Report EUR 2490.e, 1965.
- [2] A. Campanile, G. Galimi, M. Goffi, "Investigation of burnout heat flux in a double adjacent and communicating channels test section with transversely varying heat generation", Contribution to the Round Table of the European Two-Phase Flow Group - Section 4.1. - C.C.R. Ispra, 14 - 17 June 1966.

TABLE I

Burn-out data: heating on burnout rod only.

Run	Pressure ata	Flow l/h	Mass flow rate gr/cm ² sec	Inlet subcooling °C	Inlet temperature °C	Power kW	$\Phi_{B.O.}$ Watt/cm ²
18(21-2-67)	132	880	51.6	93.7	236.7	49.6	262.3
58(26-7-67)	132	855	50.1	92.7	237.7	47.4	250.7
74(7-12-66)	130	943	52.2	60.3	269	43.1	228.0
120(26-7-67)	132	1030	53.9	38.0	292.5	33.8	178.8
56(9-12-66)	131	1020	51.9	27.6	302.3	34.0	179.8
64(21-2-67)	133	2650	154.6	91.1	240	71.2	376.6
74(18-1-67)	132	2640	152.4	84.2	246.2	63.0	333.2
28(19-7-67)	132	2670	154.2	83.7	246.7	66.4	351.2
22(19-7-67)	132	2670	152.3	76.7	253.7	64.4	340.6
45(7-12-66)	130	2700	147.9	55.8	273.5	58.2	307.8
69(24-7-67)	134	2800	153.5	57.9	273.7	57.9	301.5
106(26-7-67)	132	3060	155.7	28.2	302.2	47.2	249.6
49(9-12-66)	132.5	3195	160.9	25.6	305.3	44.3	234.3

Follows Table I.

Run	Pressure ata	Flow l/h	Mass flow rate gr/cm ² sec	Inlet subcooling °C	Inlet temperature °C	Power kW	Φ B.O. Watt/cm ²
54(18-1-67)	133	3180	155.8	18.1	313.0	41.0	216.9
45(26-7-67)	132	3880	228.1	94.2	236.2	84.1	444.8
50(21-2-67)	131.5	3800	219.6	84.9	245.2	83	439.0
90(7-12-67)	132	3875	214.4	61.3	269.2	71.2	376.6
81(26-7-67)	132	4325	219.8	27.8	302.6	53.5	283.0
6(21-2-67)	132	4400	221.9	26.0	304.5	50.8	268.7
28(9-12-66)	132	4670	230.0	18.7	311.8	48.7	257.6

TABLE II

Burn-out data: heating on both rods.

Run	Pressure ata	Flow l/h	Mass flow rate gr/cm ² sec	Inlet subcooling °C	Inlet temperature °C	Total power kW	B.O. rod power kW	$\Phi_{B.O.}$ Watt/cm ²	$\frac{\Phi_A}{\Phi_{B.O.}}$
22(21-7-67)	134	870	50.6	88.6	243	73.4	46	243.3	0.595
48(21-7-67)	135	900	50.3	85.7	264.5	66.5	41.9	221.6	0.587
58(24-7-67)	134	2800	151.7	52.3	279.3	94.2	57.3	303.1	0.644
40(21-7-67)	134	3910	221.4	73.8	257.8	119.4	74.8	395.6	0.596
58(21-7-67)	136	4010	221.4	62.3	270.5	111.2	69.3	366.5	0.604
17(26-7-67)	133	850	50.0	95.1	236.0	84.1	46.3	244.9	0.816
30(26-7-67)	133	2610	151.2	85.8	245.2	122.9	67.1	354.9	0.832
44(24-7-67)	134	2830	154.5	56.1	275.5	107.8	59.2	313.1	0.821
40(26-7-67)	131	3890	227.7	91.1	238.7	153	82.8	437.9	0.848
16(24-7-67)	132	840	49.4	95.0	235.5	92.3	47.1	249.1	0.959
81(21-7-67)	133	950	53.1	66.3	264.7	80.1	40.8	215.8	0.963
89(21-7-67)	136	1015	53.3	41.5	291.2	66.2	33.9	179.3	0.953
23(24-7-67)	130	2640	152.4	82.3	247.0	130.3	66.7	352.8	0.953

Follows Table II.

Run	Pressure ata	Flow l/h	Mass flow rate gr/cm ² sec	Inlet subcooling °C	Inlet temperature °C	Total power kW	B.O. rod power kW	$\Phi_{B.O.}$ Watt/cm ²	$\frac{\Phi_A}{\Phi_{B.O.}}$
48(20-7-67)	134	2640	150.1	75.9	255.7	127.4	64.6	341.7	0.972
62(20-7-67)	134	2930	160.5	57.6	274.0	117.2	59.3	313.6	0.976
74(20-7-67)	134.5	3350	163.8	17.7	314.2	83.5	42.6	225.3	0.960
35(24-7-67)	131	3840	224.6	90.6	239.2	168.0	85.1	450.1	0.974
67(21-7-67)	134	3980	217.3	56.1	275.5	132.0	65.8	348.0	1.006
96(21-7-67)	132	4430	221.3	22.5	308.0	100.6	51	269.7	0.972

TABLE III

Burn-out data: heating on the B.O. rod and on the shell.

Run	Pressure ata	Flow l/h	Mass flow rate gr/cm ² sec	Inlet subcooling °C	Inlet temperature °C	Total power kW	B.O. rod power kW	$\Phi_{B.O.}^2$ Watt/cm ²	$\frac{\Phi_S}{\Phi_{B.O.}}$
53(3-7-67)	130	2435	139.6	78.3	251.0	119.9	57.4	303.6	0.445
5(3-7-67)	132	2440	138.0	72.0	258.4	112.2	53.5	283.0	0.452
6(3-7-67)	132	2630	145.5	60.9	269.6	112.3	52.6	278.2	0.480
35(3-7-67)	134.5	3010	151.0	24.9	307.0	85.0	40.3	213.1	0.460
50(3-7-67)	135.5	2980	135.5	16.7	315.8	73.3	34.7	183.5	0.450
47(13-7-67)	133	2330	135.0	86.1	245.0	161.6	55.3	292.5	0.835
58(13-7-67)	132	2535	141.0	64.0	266.5	143.8	49.3	260.7	0.830
16(13-7-67)	134	2570	140.6	57.1	274.5	134.7	47.1	249.1	0.831
40(13-7-67)	132	2770	138.8	23.5	307.0	110.0	38.0	201.0	0.838
32(13-7-67)	134	2980	136.4	2.45	329.2	88.0	30.2	159.7	0.848

TABLE IV

Burn-out data: heating on both rods and on the shell.

Run	Pressure ata	Flow l/h	Mass flow rate gr/cm ² sec	Inlet subcooling °C	Inlet temperature °C	Total power kW	B.O. rod power kW	$\Phi_{B.O.}$ Watt/cm ²	$\frac{\Phi_A}{\Phi_{B.O.}}$	$\frac{\Phi_S}{\Phi_{B.O.}}$
10(19-1-67)	133.5	2600	148.6	79.1	252.2	133.8	55.5	293.5	0.434	0.419
24(19-1-67)	134.5	2744	150.7	59.9	272.0	121.1	50.2	265.5	0.436	0.415
37(19-1-67)	136	2975	156.4	42.3	290.5	113.1	46.9	248.1	0.437	0.412
47(19-1-67)	135	3316	158.6	12.7	319.5	87.6	35.9	189.9	0.465	0.407
40(17-1-67)	129.5	2750	153.6	64.9	263.7	149	51.6	272.9	0.581	0.555
91(17-1-67)	134.5	3036	156.0	33.2	298.7	122.3	42.5	224.8	0.579	0.541
117(17-1-67)	134	3210	155.0	14.6	317.0	97.1	34.2	180.9	0.567	0.539
50(14-7-67)	133	2370	135.5	78.3	252.7	198.1	51.0	269.7	0.890	0.856
74(14-7-67)	135	2460	132.7	51.5	280.7	168.4	43.7	231.1	0.883	0.820
88(14-7-67)	134	2750	140.4	30.1	301.5	149.2	38.9	205.7	0.872	0.819
95(14-7-67)	141	2770	137.0	23.9	311.7	135.9	35.2	186.2	0.872	0.823

Follows Table IV.

Run	Pressure ata	Flow l/h	Mass flow rate gr/cm ² sec	Inlet subcooling °C	Inlet temperature °C	Total power kW	B.O. rod power kW	$\Phi_{B.O.}$ Watt/cm ²	$\frac{\Phi_A}{\Phi_{B.O.}}$	$\frac{\Phi_S}{\Phi_{B.O.}}$
13(19-7-67)	130	2630	151.0	81.3	248.0	212.7	54.9	290.4	0.903	0.852
47(18-1-67)	132	2952	156.0	42.2	288.3	167.0	43.9	232.2	0.863	0.823
22(18-1-67)	135	3100	160.9	37.1	295.1	158.6	41.7	220.5	0.868	0.815
38(18-1-67)	139	3180	154.2	18	316.5	130.9	34.4	181.9	0.869	0.808

TABLE V

Burn-out data heating on both rods.

Run	Pressure ata	Flow l/h	Mass flow rate gr/cm ² sec	Inlet subcooling °C	Inlet temperature °C	Total power kW	B.O. rod power kW	$\Phi_{B.O.}$ Watt/cm ²	$\frac{\Phi_A}{\Phi_{B.O.}}$
7(20-7-67)	52.5	1775	110.7	75.7	190.0	158.6	79.3	419.4	1
18(20-7-67)	53	1785	106.4	44.3	222.0	134.2	68.2	360.7	0.968
30(20-7-67)	55	1890	107.7	20.0	248.7	113.4	57.6	304.6	0.969
74(2-8-67)	53	1975	110.7	9.6	256.7	74.6	39	206.3	0.913

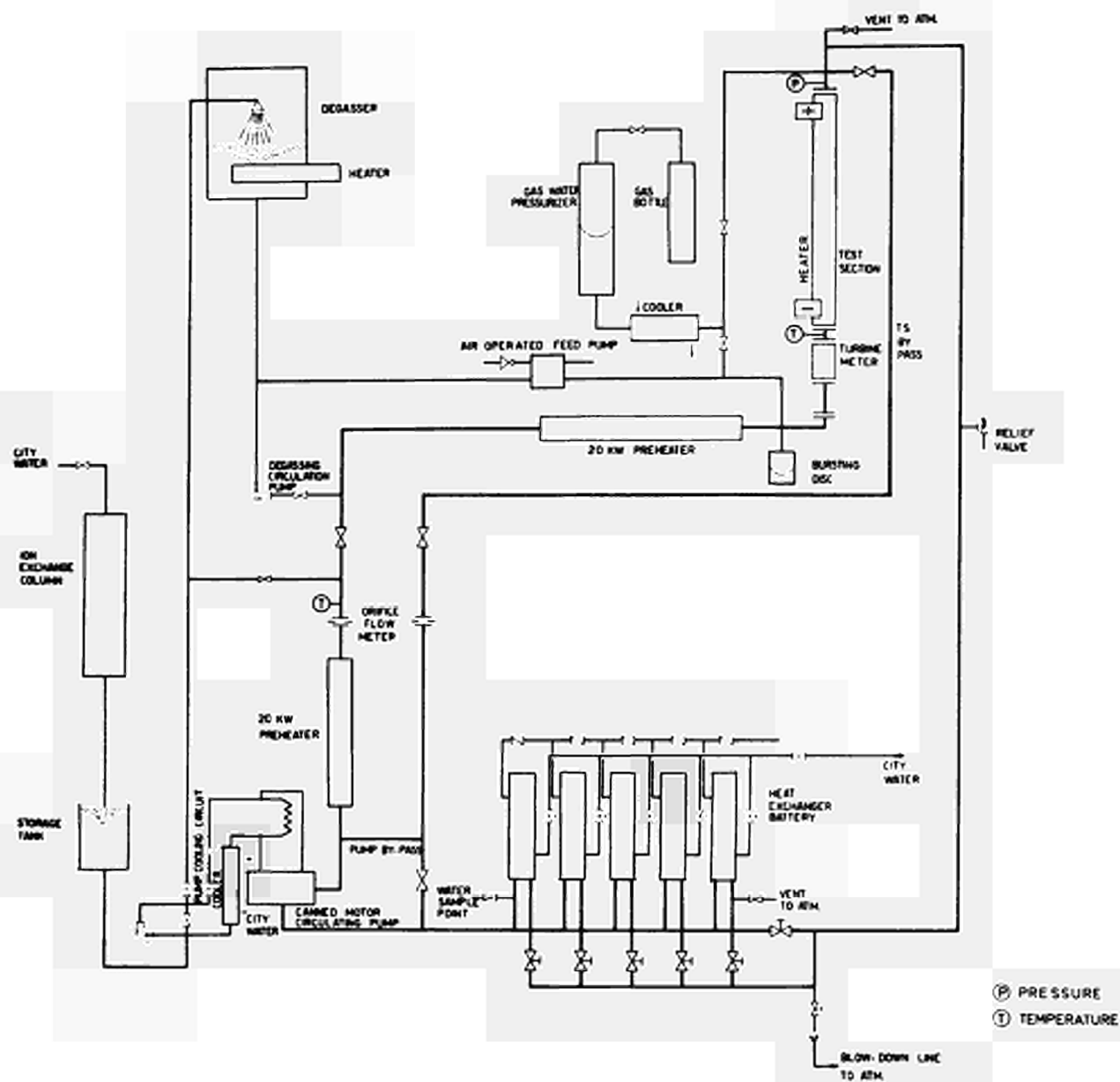


Fig. 1 - Flow diagram.

SORIN
SALUGGIA

SEZIONE DI PROVA N°4
CONTORNO DEL CANALE RISCALDATO.

SCALA
15:1

DATA
1964

DIS. *FP.*

N.°
SDM-971

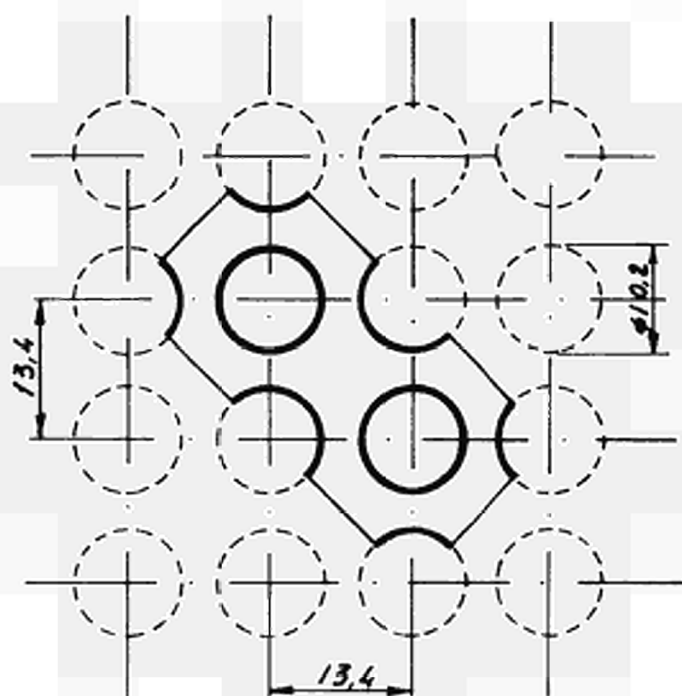


Fig. 2 - Cross section of flow passage.

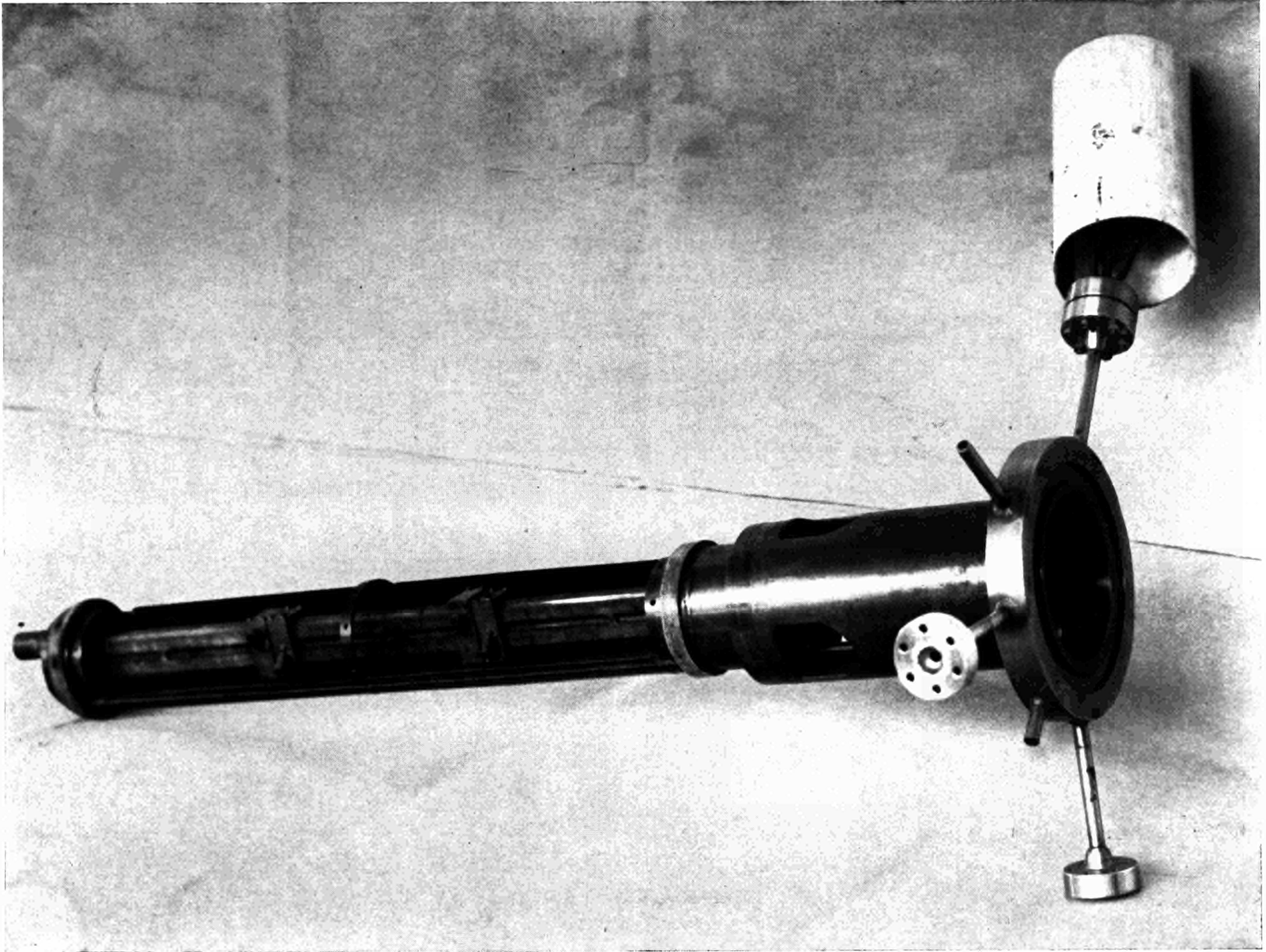


Fig. 3 — Close-up view of the channel showing the location of the spacers.

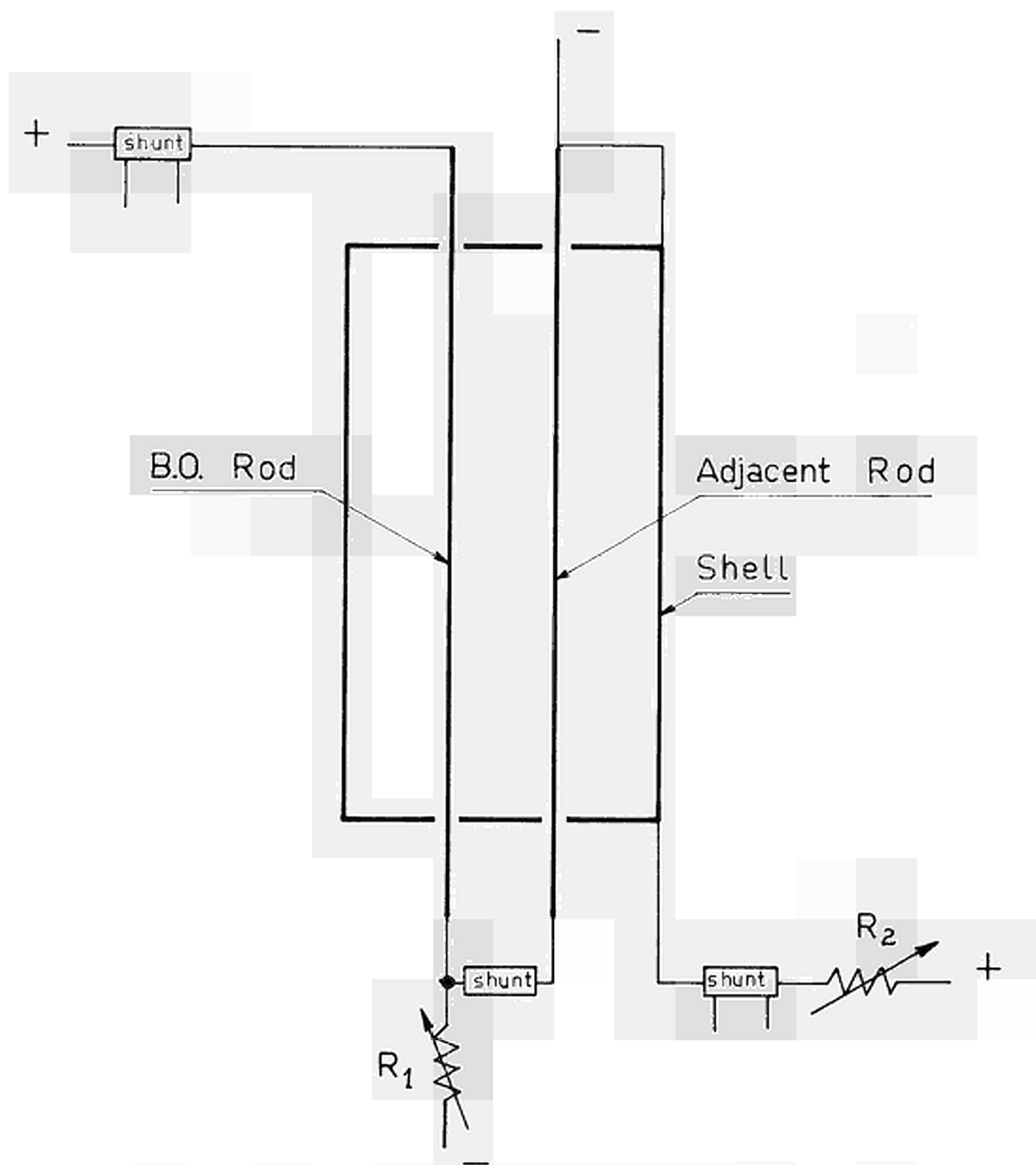
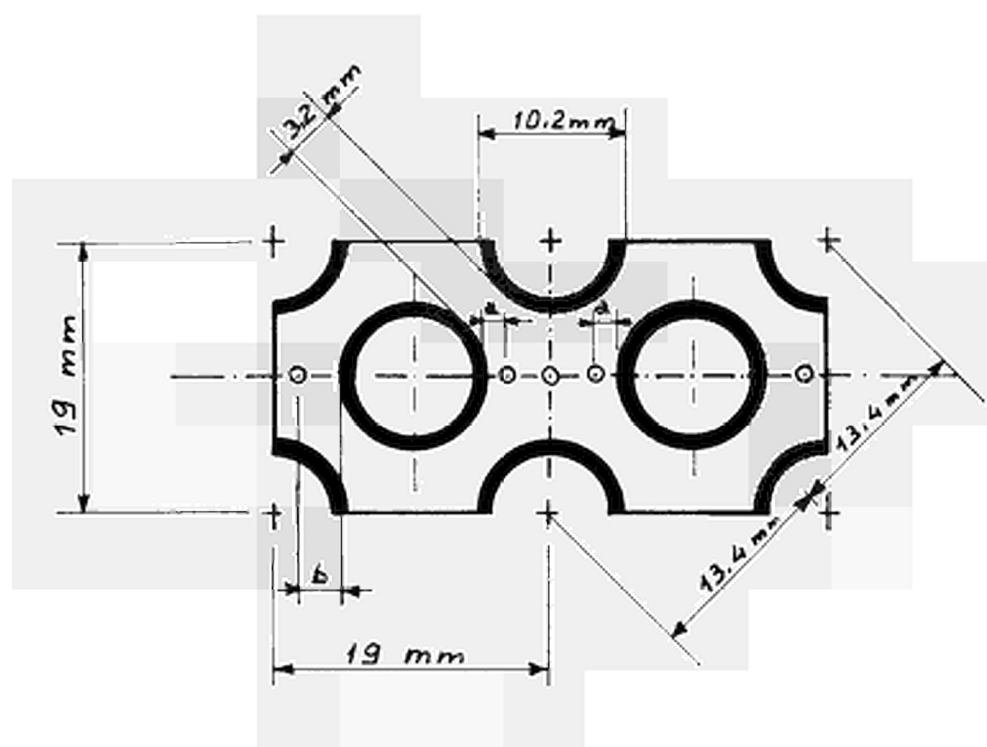


Fig. 4 - Schematic diagram of the electrical connection arrangement.



Fig. 5 — Close-up view of the exit section of the channel.



$$a = 1,5 \text{ mm}$$

$$b = 2,9 \text{ mm}$$

Fig. 6 - Relevant dimensions of the flow passage showing the positions of the exit water temperature probes.

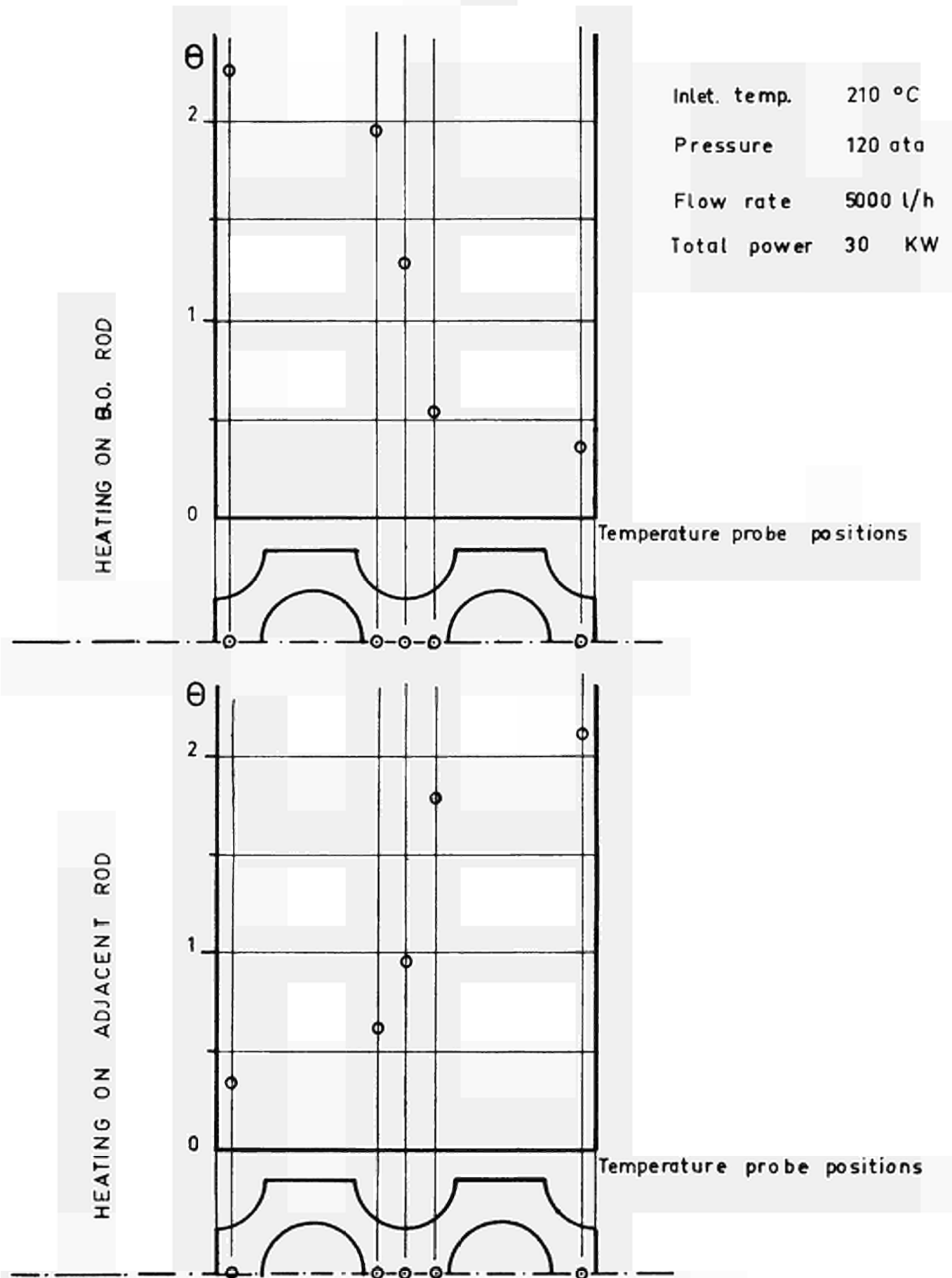


Fig. 7 - Transverse coolant temperature rise for several points of the exit section during tests for control of the subchannels geometrical symmetry: Asymmetrical heating.

Inlet temperature	202 °C
Pressure	110 ata
Flow rate	2875 l/h
Total power	62,7 KW

HEATING ON BOTH RODS

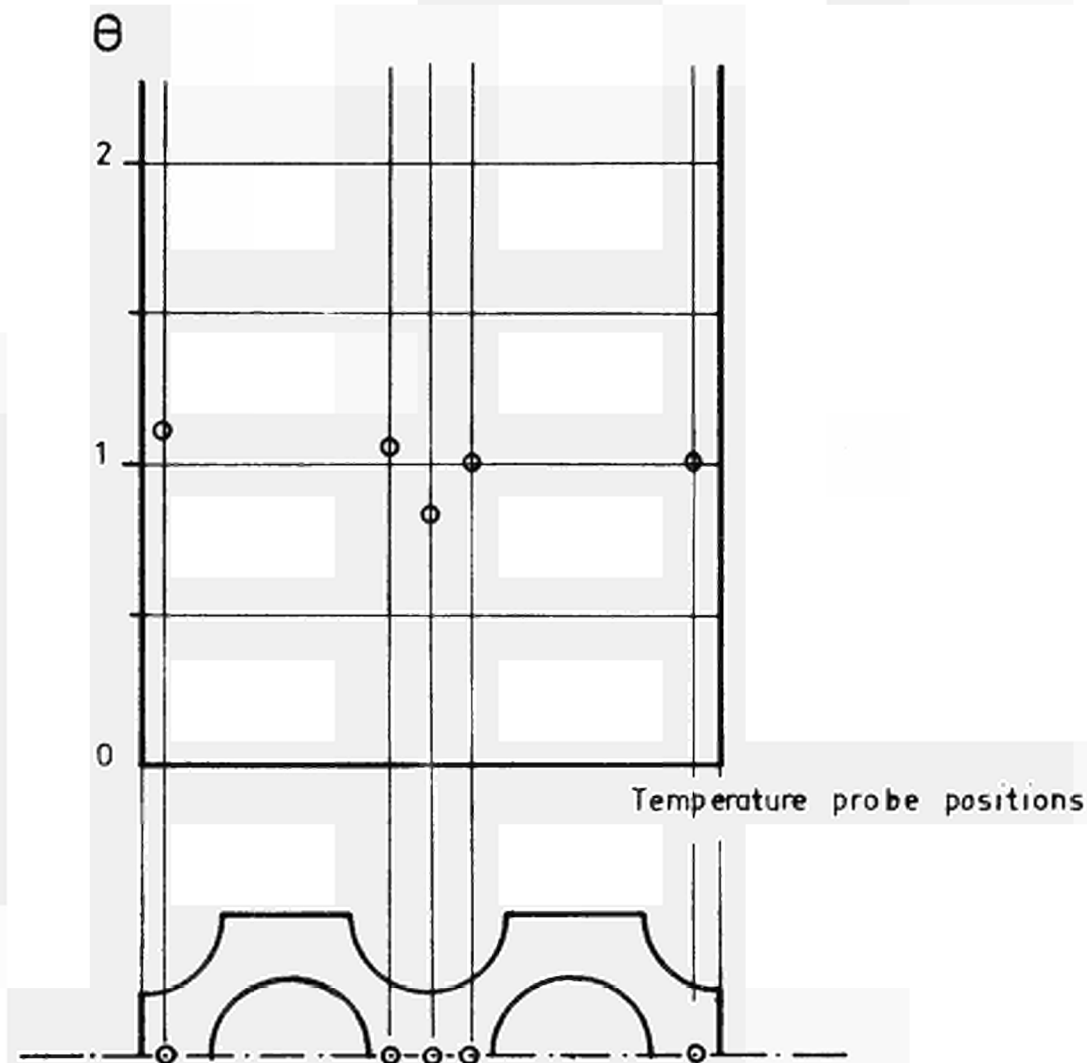


Fig. 8 - Transverse coolant temperature rise for several points of the exit section during tests for control of the subchannels geometrical symmetry: Symmetrical heating.

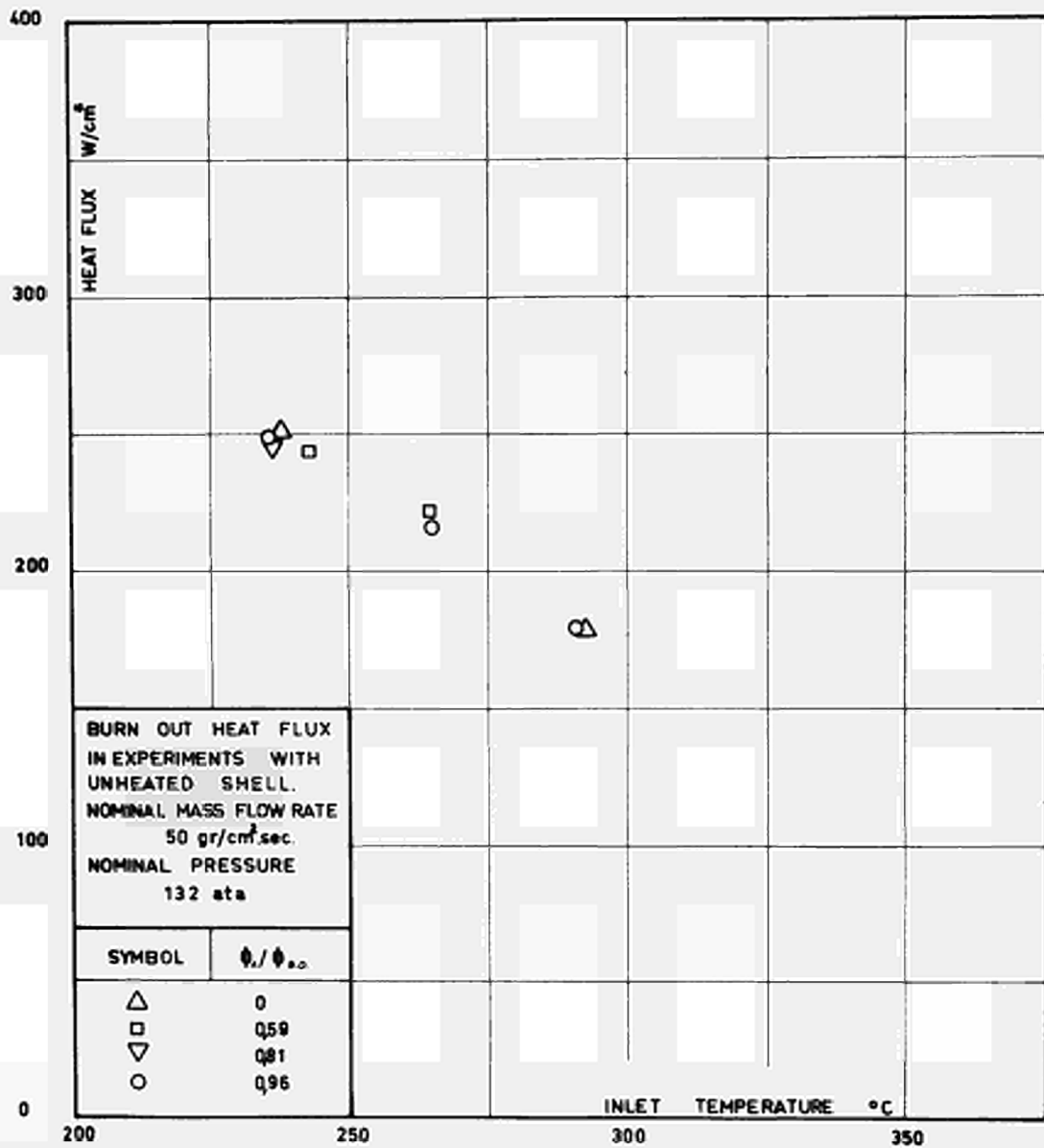


Fig. 9 - Burnout heat flux in experiments with unheated shell.
Nominal mass flow rate 50 gr/cm²sec
Nominal pressure 132 ata

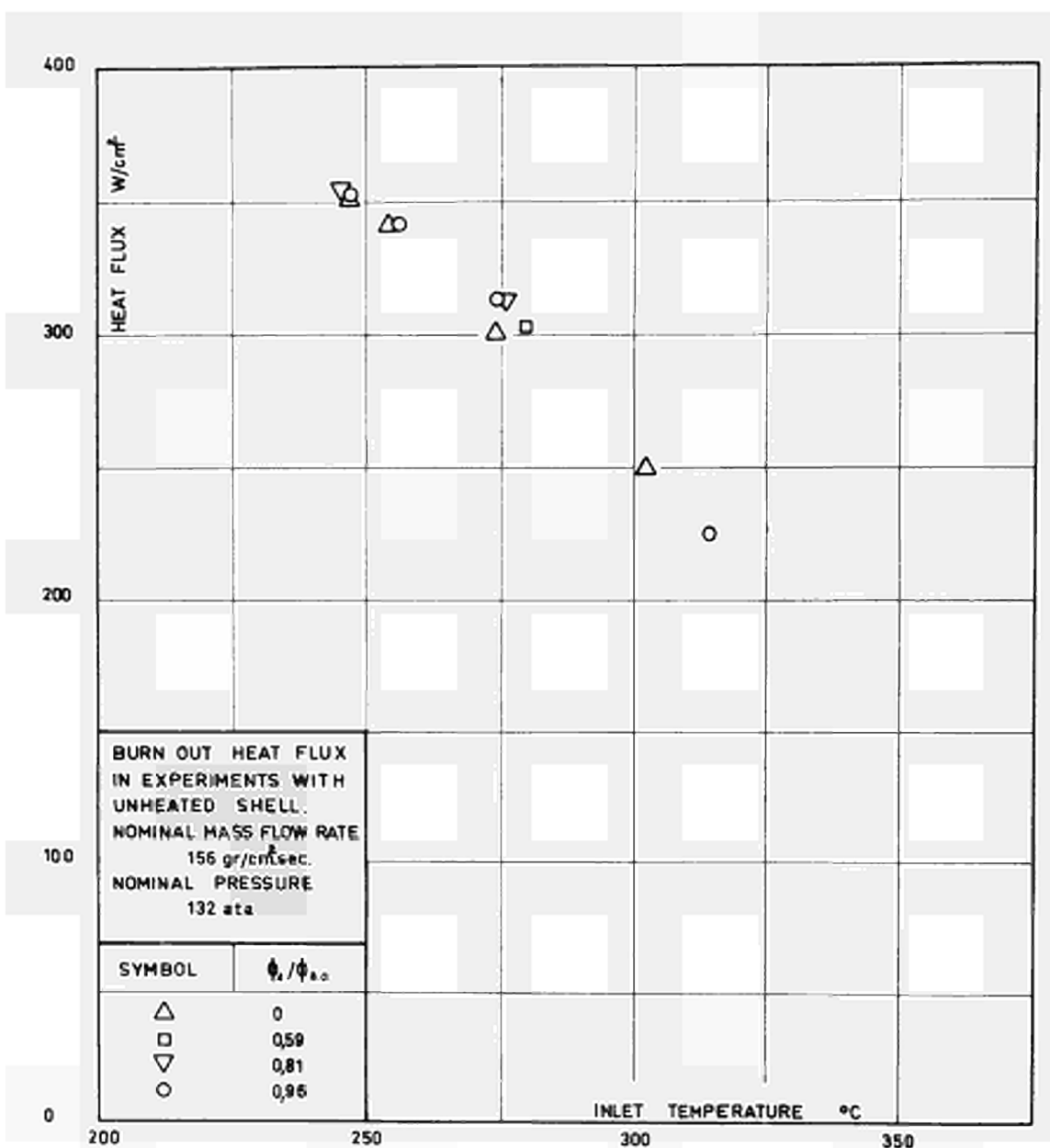


Fig. 10 - Burnout heat flux in experiments with unheated shell.

Nominal mass flow rate 156 gr/cm²sec
 Nominal pressure 132 ata

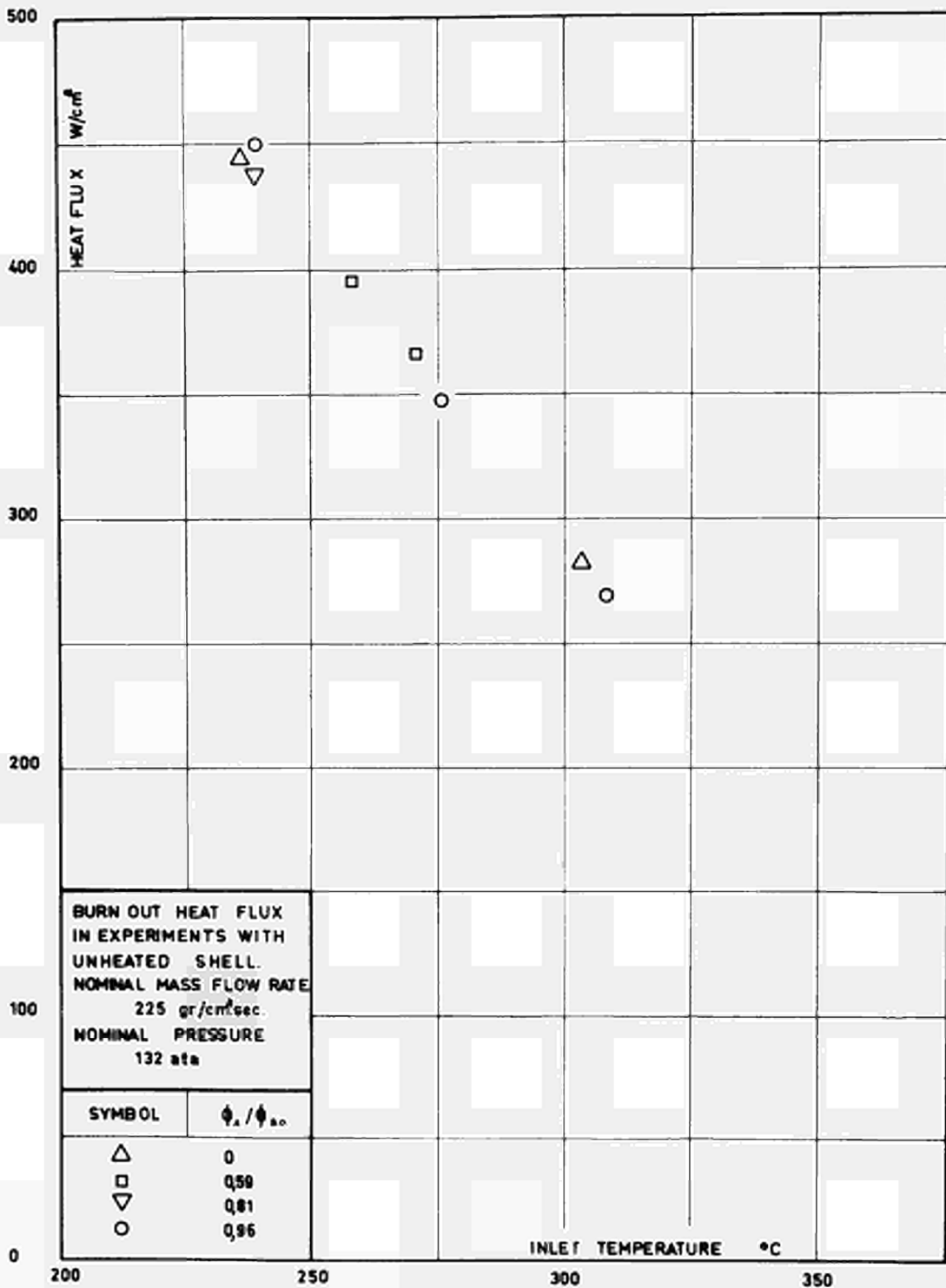


Fig. 11 - Burnout heat flux in experiments with unheated shell.

Nominal mass flow rate 225 gr/cm²sec
 Nominal pressure 132 ata

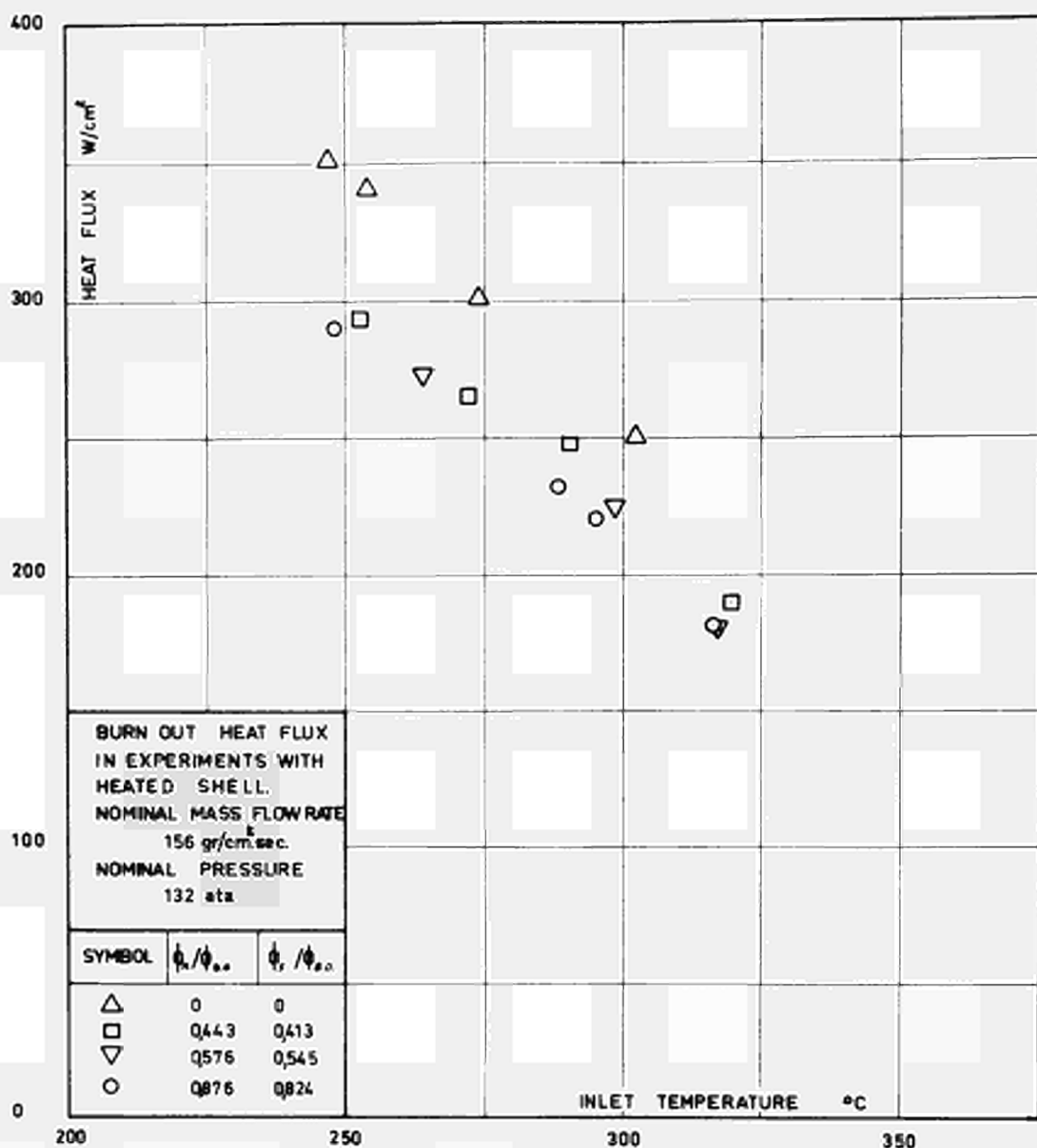


Fig. 12 - Burnout heat flux in experiments with heated shell.
Nominal mass flow rate 156 gr/cm²sec
Nominal pressure 132 ata

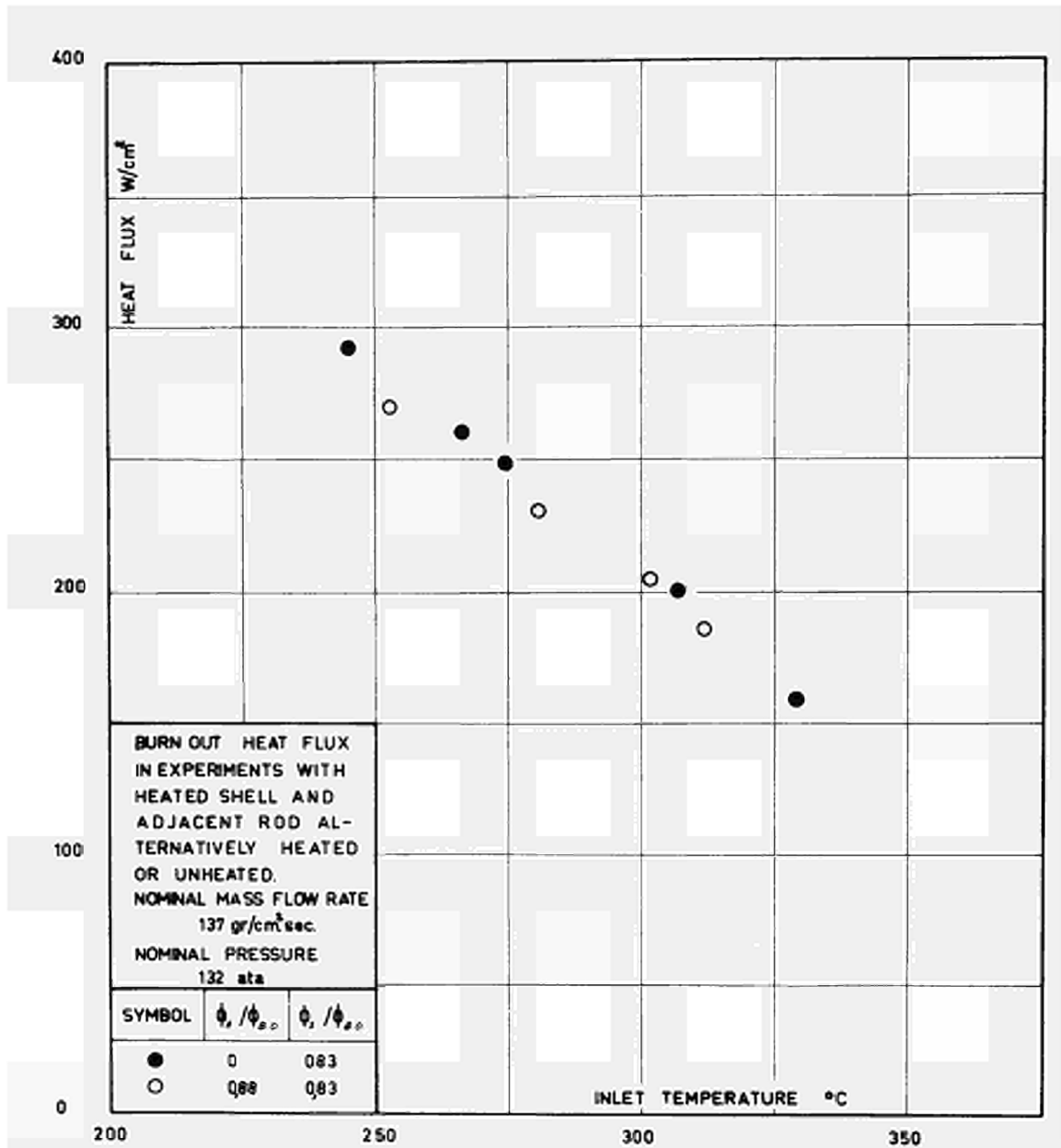


Fig. 13 - Burnout heat flux in experiments with heated shell and adjacent rod alternatively heated or unheated.
Nominal mass flow rate 137 gr/cm²sec
Nominal pressure 132 ata

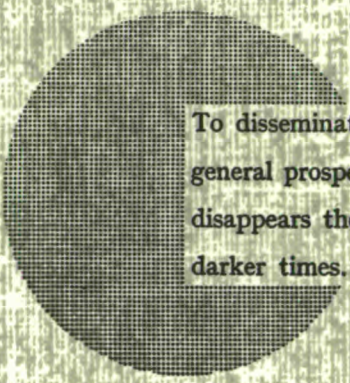
NOTICE TO THE READER

All Euratom reports are announced, as and when they are issued, in the monthly periodical **EURATOM INFORMATION**, edited by the Centre for Information and Documentation (CID). For subscription (1 year: US\$ 15, £ 5.7) or free specimen copies please write to:

Handelsblatt GmbH
"Euratom Information"
Postfach 1102
D-4 Düsseldorf (Germany)

or

Office central de vente des publications
des Communautés européennes
2, Place de Metz
Luxembourg



To disseminate knowledge is to disseminate prosperity — I mean general prosperity and not individual riches — and with prosperity disappears the greater part of the evil which is our heritage from darker times.

Alfred Nobel

SALES OFFICES

All Euratom reports are on sale at the offices listed below, at the prices given on the back of the front cover (when ordering, specify clearly the EUR number and the title of the report, which are shown on the front cover).

OFFICE CENTRAL DE VENTE DES PUBLICATIONS DES COMMUNAUTES EUROPEENNES

2, place de Metz, Luxembourg (Compte chèque postal N° 191-90)

BELGIQUE — BELGIË

MONITEUR BELGE
40-42, rue de Louvain - Bruxelles
BELGISCH STAATSBAD
Leuvenseweg 40-42 - Brussel

LUXEMBOURG

OFFICE CENTRAL DE VENTE
DES PUBLICATIONS DES
COMMUNAUTES EUROPEENNES
9, rue Goethe - Luxembourg

DEUTSCHLAND

BUNDESANZEIGER
Postfach - Köln 1

NEDERLAND

STAATSDRUKKERIJ
Christoffel Plantijnstraat - Den Haag

FRANCE

SERVICE DE VENTE EN FRANCE
DES PUBLICATIONS DES
COMMUNAUTES EUROPEENNES
26, rue Desaix - Paris 15^e

ITALIA

LIBRERIA DELLO STATO
Piazza G. Verdi, 10 - Roma

UNITED KINGDOM

H. M. STATIONERY OFFICE
P. O. Box 569 - London S.E.1

EURATOM — C.I.D.
51-53, rue Belliard
Bruxelles (Belgique)